

TYC 1031 1262 1^{*}: An Anomalous Cepheid in a double-lined eclipsing binary

E. Sipahi¹†, C. İbanoğlu¹, Ö. Çakırlı¹, S. Evren¹

¹*Ege University, Science Faculty, Astronomy and Space Sciences Dept., 35100 Bornova, İzmir, Turkey*

24 June 2018

ABSTRACT

Multi-color light curves and radial velocities for TYC 1031 1262 1 have been obtained and analyzed. TYC 1031 1262 1 includes a Cepheid with a period of 4.15270 ± 0.00061 days. The orbital period of the system is about 51.2857 ± 0.0174 days. The pulsation period indicates a secular period increase with an amount of 2.46 ± 0.54 min/yr. The observed B, V, and R magnitudes were cleaned for the intrinsic variations of the primary star. The remaining light curves, consisting of eclipses and proximity effects, are obtained and analyzed for orbital parameters. The system consists of two evolved stars, F8II+G6II, with masses of $M_1 = 1.640 \pm 0.151 M_{\odot}$ and $M_2 = 0.934 \pm 0.109 M_{\odot}$ and radii of $R_1 = 26.9 \pm 0.9 R_{\odot}$ and $R_2 = 15.0 \pm 0.7 R_{\odot}$. The pulsating star is almost filling its corresponding Roche lobe which indicates the possibility of mass loss or transfer having taken place. We find an average distance of $d = 5070 \pm 250$ pc using the BVR and JHK magnitudes and also the V-band extinction. Kinematic properties and the distance to the galactic plane with an amount of 970 pc indicate that it belongs to the thick-disk population. Most of the observed and calculated parameters of the TYC 1031 1262 1 lead to a classification of an Anomalous Cepheid.

Key words: stars: binaries: eclipsing – stars: fundamental parameters – stars: binaries: spectroscopic – stars: variables: Cepheids

* Based on the data obtained at TÜBİTAK National Observatory

† e-mail: esin.sipahi@mail.ege.edu.tr

1 INTRODUCTION

Pulsating variables are located in a restricted region, so-called Cepheid instability strip (IS) in the Hertzsprung-Russell (HR) diagram. This region includes δ Scuti, RR Lyrae, Population I and II Cepheids which represent an important testing basis for theories on stellar structure and evolution as well as pulsation mechanisms. These variables have very different masses, effective temperatures and chemical abundances. The stars in the IS are found not only in a wide range of masses but also found among very young Population I type stars to very old Population II type stars. These stars in the IS reveal many properties of the stellar interiors.

At the beginning of the 20th century Miss Leavitt made a great discovery that there is a relation between the period and absolute magnitude of the Cepheid variables in the Small Magellanic Cloud. Three decades later Baade (1953) called attention to the difference in the period-luminosity (hereafter P-L) relations of the Cepheids in the globular clusters and the classical Cepheids. Thus, the Cepheids are divided into two groups which are Population I (usually called Type I Cepheids) and Population II Cepheids (or Type II Cepheids), the formers are about 1.5 mag brighter than the latter for the same pulsation periods. Taking into account this difference Blaauw & Morgan (1954) made a revision on the P-L relation for the classical Cepheids. These variables are still used as distance indicators not only for our galaxy but also for nearby spiral and irregular galaxies. While the Type I Cepheids are young-disk stars associated with spiral arm and thin-disk populations evolved from main-sequence stars with masses from 3 to 15 solar masses, Type II Cepheids can be old-disk, thick-disk, or halo stars with masses somewhat smaller than the Sun (see Wallerstein (2002), and references therein). Type II Cepheids are divided into three subclasses regarding their pulsation periods: BL Her stars with a period of < 7 d, W Vir stars with $7 < P < 20$ d and RV Tau type variables with $P > 20$ d. Recently Soszynski et al. (2008) suggested divisions at 4 and 20 days. Masses and radii for these stars were estimated from their pulsation properties. BL Her stars are common in globular clusters and in the disk of our galaxy. Harris (1981) showed that four of the 12 field BL Her stars have [Fe/H] values less than -1.5 which were identified as halo objects with a mean distance from the galactic plane of 1.8 kpc. In contrary, the 8 stars have metallicities near or above solar values. Their mean distance from the Galactic plane was about 0.25 kpc, indicating characteristic of thick or thin-disk population. There are some metal-poor variables with periods between 0.5 and 3 or more days lying above the RR Lyrae-type stars which may have entirely different origin as compared to the normal Type II Cepheids in the globular clusters. These variables are called as Anomalous Cepheids (hereafter ACs). They are found in

the general field, globular clusters and nearby dwarf spheroidal galaxies. Anomalous Cepheids are brighter than the Type II Cepheids at fixed color, and hence they follow a different P-L relation (Soszynski et al. 2008). Fiorentino et al. (2006) (and references therein) suggested that the ACs are extension of the Type I Cepheids to lower metallicities and masses. Moreover, they predict a mass range for the ACs as $1.9 < M/M_{\odot} < 3$, which may be a product of a mass about $M < 4 M_{\odot}$, experienced the helium flash in the past.

Only six Type II Cepheids were known to be spectroscopic binaries. TX Del, IX Cas, AU Peg and ST Pup are single-lined binaries for which spectroscopic observations and the resultant orbits were published. Due to low orbital inclination no eclipses were detected in these binaries. Recently, two Cepheid variables in eclipsing binaries, namely TYC 1031 1262 1 and NSV 10993, were discovered by Antipin, Sokolovski & Ignatieva (2007) and Khruslov (2008). The pulsation periods are nearly identical with an amount of 4.2 d, but the orbital periods are about 51 and 40 days. In the second part of the OGLE-III catalog of Variable stars Soszynski et al. (2008) presented 197 Type II Cepheids of which seven are eclipsing variables and 83 ACs in the Large Magellanic Cloud. Since masses and radii for the stars were measured directly from the eclipse light curves and radial velocities, a detailed study of these Cepheids in the eclipsing binaries would be well worthwhile.

The light variability of TYC 1031 1262 1 (ASAS J182611+1212.6, 2MASS J18261150+1212349, GSC 01031-01262, $V=11^m.64$, $B-V=0^m.77$) was discovered by Pojmanski, Pilecki & Syczygiel (2005) during the All-Sky Automated Survey (ASAS-3). The variability of this star was also detected independently by Antipin, Sokolovski & Ignatieva (2007) on Moscow archive plates in Crimea. They plotted the observations obtained by ASAS-3, photographic magnitudes obtained from the plates taken with the 40 cm astrograph in the Crimea and the observations obtained by the Northern Sky Variability Survey (NSVS, Wozniak et al. (2004)) against the time and noticed a new variable as a Cepheid with some peculiarities. They started observations of TYC 1031 1262 1 with the 50 cm telescope of the Crimean Laboratory. These CCD observations clearly revealed eclipsing nature of the star with a Type II Cepheid component in our Galaxy. The pulsation and orbital periods are estimated to be 4.1523 and 51.38 d, respectively. Schmidt et al. (2009) made VR photometry of Cepheid variable star candidates including TYC 1031 1262 1 in 2005 and 2006. They proposed a pulsation period of about 4.1508 d and classified it as a Type I Cepheid.

In this study we present our multi-color photometric and spectroscopic observations of TYC 1031 1262 1. The main aim of this study is to derive the masses and radii of the components. Thus, mass and radius of a Type II Cepheid will be revealed, for the first time, directly from the spectroscopic and

photometric observations. We will also discuss the pulsation characteristics and its place in our Galaxy.

2 OBSERVATIONS

2.1 Photometric observations

The photometric observations in the wide-band Johnson UBVR system were carried out with the 48 cm Cassegrain reflecting telescope and 35 cm MEADE LX200 GPS telescope at the Ege University Observatory. In the observations with the 48 cm telescope High-Speed Three-Channel Photometer and standard UBVR passbands were used. Thermoelectrically cooled ALTA U+42 2048x2048 pixel CCD camera including BVR passbands was attached to Schmidt Cassegrain type Meade telescope. The BVR observations in 2008 were obtained on 63 nights between March 2 and November 5. The observations in 2009 were obtained on 17 nights between August 3 and October 8. GSC 1031 193 and GSC 1031 1445 are taken as the comparison and check stars, respectively. Some basic parameters of the comparison stars taken from the SIMBAD database are listed in Table 1. Although the program and comparison stars are very close in the sky, differential atmospheric extinction corrections were applied, especially for the observations obtained with the 48 cm telescope. While all the program stars were observed simultaneously with the 35 cm telescope, each star was observed successively with the 48 cm telescope, i.e. in different times. The atmospheric extinction coefficients were obtained from observations of the comparison stars on each night. Moreover, the comparison stars were observed with the standard stars in their vicinity and reduced differential magnitudes, in the sense variable minus comparison, were transformed to the standard system. The standard stars are chosen from the lists of Landolt (1983, 1992). Heliocentric corrections were also applied to the times of the observations.

In Fig. 1 we plot the U-, B-, V- and R-passband observations versus the pulsation period of the Cepheid variable. As it is seen the dominant light variations are originated from the pulsation. The below shifted observations correspond to the eclipses. The standard deviations of each data point are about 0.05, 0.03, 0.01, and 0.01 mag in U, B, V and R passbands, respectively. The observational data can be obtained from the authors.

2.2 Spectroscopic observations

Optical spectroscopic observations of TYC 1031 1262 1 were obtained with the Turkish Faint Object Spectrograph Camera (TFOSC) attached to the 1.5 m telescope on 6 nights (July-October,

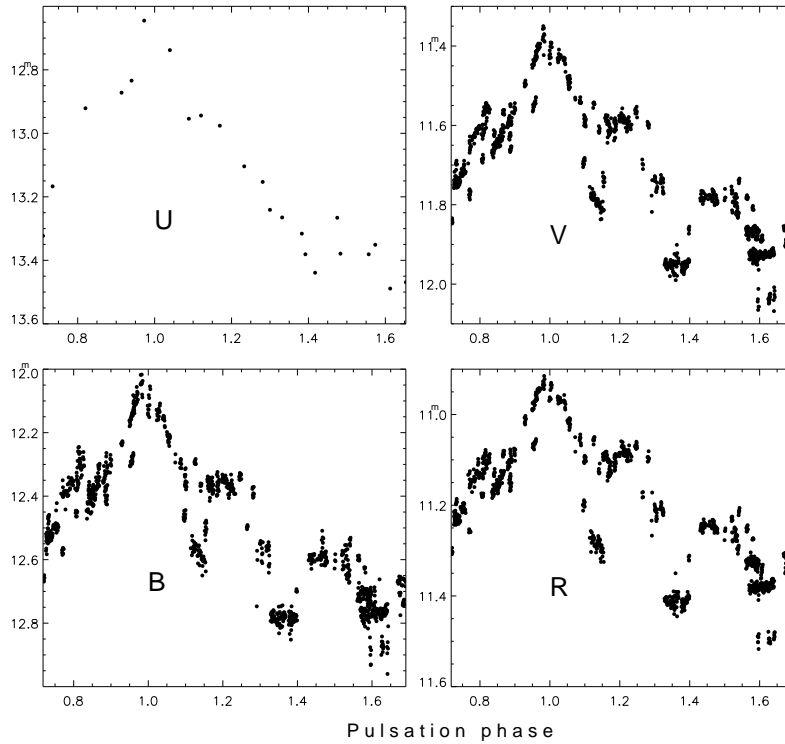


Figure 1. The U-, B-, V-, and R-passband light curves for TYC 1031 1262 1. The ordinates and abscissae are the standard magnitudes and the pulsation phases.

Table 1. The coordinates, apparent visual magnitudes and the colors of the stars observed.

Star	α	δ	V (mag)	B-V(mag)
TYC 1031 1262 1	$18^h 26^m 11.5^s$	$12^\circ 12' 34''.8$	11.64	0.77
GSC 1031 193	18 26 23.7	12 15 47.2	10.99	0.66
GSC 1031 1445	18 26 04.9	12 07 11.6	10.44	0.63

2011) under good seeing conditions. Further details on the telescope and the spectrograph can be found at <http://www.tug.tubitak.gov.tr>. The wavelength coverage of each spectrum was 4000-9000 Å in 12 orders, with a resolving power of $\lambda/\Delta\lambda$ 7000 at 6563 Å and an average signal-to-noise ratio (S/N) was ~ 120 . We also obtained a high S/N spectrum of the α Lyr (A0 V) and HD 50692 (G0V) for use as templates in derivation of the radial velocities (Nidever et al. 2002).

The electronic bias was removed from each image and we used the 'creject' option for cosmic ray removal. Thus, the resulting spectra were largely cleaned from the cosmic rays. The echelle spectra were extracted and wavelengths were calibrated by using Fe-Ar lamp source with help of the IRAF ECHELLE (Tonry & Davis 1979) package.

The stability of the instrument was checked by cross-correlating the spectra of the standard

star against each other using the FXCOR task in IRAF. The standard deviation of the differences between the velocities measured using FXCOR and the velocities in Nidever et al. (2002) was about 1.1 km s^{-1} .

3 PULSATION AND ORBITAL PERIODS

3.1 Pulsation period

The pulsation period was estimated by Antipin, Sokolovski & Ignatieva (2007) and Schmidt et al. (2009) as 4.1523 and 4.1508 d, respectively. Since the light variation of the pulsating component dominates in the light curve we first attempted to refine the pulsation period using the program PERIOD04 (Lenz & Breger 2005). A Fourier power spectrum of all the available V-passband data gave a spectral peak at a frequency about $f_0=0.2409 \text{ c/d}$ which corresponds to 4.1581 d. This package computes amplitudes and phases of the dominant frequency as well as simultaneous multi-frequency sine wave fitting. Since the observations were obtained with different instruments in different years under dissimilar observing conditions, many systematic observational errors and computational errors affected the data. Therefore, we did not attempt to search for the second or the third frequencies for pulsation if they really do exist. As it will be explained in §4 we represented all available V-data, subtracting the eclipses, with a truncated Fourier series which includes cosine and sine terms up to second order. We then calculated the light variation originated from the oscillations of the more luminous component. We separated all the data with an interval of about 6 days and determined maximum times by shifting the calculated light curve along the time axis. It should be noted here that the shape of the light curve is assumed to be more or less constant during the time base of the observations. After the best fit is obtained, the times for the mid-maximum light are read off directly from the observations and presented in Table 2. Although the observations obtained by ASAS and AAVSO have relatively large scatters we had to use all the data because of limited observations both in time elapsed and the continuous observations due to its relatively longer pulsation period. Using the ephemeris given by Antipin, Sokolovski & Ignatieva (2007)

$$\text{Max}(HJD) = 2\,453\,196.529 + 4^d.1523 \times E \quad (1)$$

we obtained the residuals between the observed and calculated times of mid-maximum light as well as the number of the elapsed cycles. In Fig. 2 we plot the residuals O-C(I) versus the epoch numbers. The variation of the residuals resembles a parabolic change, in other words

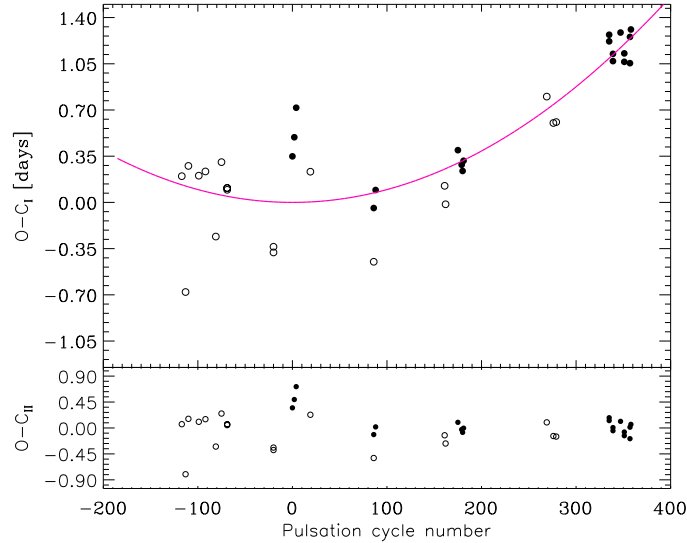


Figure 2. The O-C residuals obtained by Eq.1 for the pulsating star of TYC 1031 1262 1 are plotted against the pulsation cycle number. A parabolic fit to the data is shown by solid line. The deviations from the parabolic fit are plotted in the bottom panel. Open circles refer to ASAS and AAVSO, and the dots to the data Antipin, Sokolovski & Ignatieva (2007) and this study.

TYC 1031 1262 1 appears to be undergoing gradual period increase. A least squares solution gives the following ephemeris,

$$\text{Max}(HJD) = 2\,453\,196.201(0.061) + 4^d.15270(0.00061) \times E + 9.73(2.13)10^{-6} \times E^2 \quad (2)$$

The standard deviations in the last digits are given in the parentheses. In the bottom panel of Fig. 2 the deviations from the parabolic fit are also plotted. TYC 1031 1262 1 is undergoing period increase amounting to $2.46 (\pm 0.54) \text{ min yr}^{-1}$. Despite the fact that the data base is very short, over five years, the characteristics of the variation in the pulsation period could be revealed.

3.2 Orbital period

The orbital period of TYC 1031 1262 1 was estimated by Antipin, Sokolovski & Ignatieva (2007) as 51.38 d. We subtracted intrinsic variations of the more luminous star from all the available data, thus, the remaining light variations were assumed to be originated from the eclipses and proximity effects. We revealed light variations due to the eclipses and proximity analysis with an analysis of these data. The shape of the primary eclipse was revealed and compared by the observations which fall in the ascending and descending branches of the eclipse. Comparing the computed light curve with the observations, we obtained 28 times for mid-eclipse and presented in Table 3. The O-C(I) residuals were computed using the first ephemeris given by Antipin, Sokolovski & Ignatieva

Table 2. The times of mid-maximum light for TYC 1031 1262 1. The O-C(I) and O-C(II) residuals were computed with Eqs.1 and 2, respectively.

HJD-2 450 000	E	O-C(I)	O-C(II)	Filter	Ref.
2710.533	-117	-0.177	0.065	V	1
2726.267	-113	-1.052	-0.803	V	1
2739.680	-110	-0.096	0.158	V	1
2785.286	-99	-0.166	0.107	V	1
2814.387	-92	-0.131	0.152	V	1
2859.573	-81	-0.619	-0.323	V	1
2885.053	-75	-0.053	0.250	V	1
2909.760	-69	-0.260	0.049	V	1
2909.773	-69	-0.247	0.062	V	1
3112.768	-20	-0.672	-0.383	V	1
3112.811	-20	-0.715	-0.340	V	1
3196.529	0	0.000	0.328	V	1
3205.000	2	0.166	0.494	V	2
3213.529	4	0.391	0.717	V	2
3275.335	19	-0.088	0.229	V	2
3552.884	86	-0.743	-0.521	V	1
3553.291	86	-0.336	-0.114	V	1
3561.733	88	-0.198	0.019	V	2
3864.912	161	-0.137	-0.126	V	2
3868.925	162	-0.277	-0.269	V	1
3923.320	175	0.138	0.099	V	1
3939.820	179	0.029	-0.026	V	2
3943.926	180	-0.017	-0.076	V	2
3948.156	181	0.061	-0.002	V	2
4276.264	260	0.133	-0.297	V	2
4314.080	269	0.582	0.099	V	3
4342.949	276	0.385	-0.138	V	3
4355.414	279	0.393	-0.148	V	3
4388.986	287	0.747	0.159	V	3
4588.577	335	1.027	0.130	V	4
4588.627	335	1.077	0.180	R	4
4605.038	339	0.879	-0.046	R	4
4605.093	339	0.934	0.009	V	4
4638.476	347	1.099	0.117	V	4
4654.865	351	0.879	-0.132	R	4
4654.929	351	0.943	-0.068	V	4
4679.771	357	0.871	-0.184	R	4
4679.970	357	1.040	0.015	V	4
4684.179	358	1.127	0.064	V	4
4684.263	358	1.211	0.148	R	4

Ref: (1) ASAS, (2) Antipin, Sokolovski & Ignatieva (2007), (3) AAVSO (4) This study

(2007). In Fig. 3 we plot O-C(I) residuals versus the epoch numbers. A linear least squares fit gives the following ephemeris,

$$\text{Min}(HJD) = 2\,454\,699.964(0.279) + 51^d.2857(0.0174) \times E \quad (3)$$

The new orbital period is about 0.1 d shorter than the one estimated previously.

Table 3. The times of mid-minimum light for TYC 1031 1262 1. The O-C(I) and O-C(II) residuals were computed with the ephemeris given by Antipin, Sokolovski & Ignatieva (2007) and Eq. 3, respectively.

HJD-2 450 000	E	O-C(I)	O-C(II)	Filter	Ref.
3211.7872	-29	-8.520	-0.892	V	1
3212.8663	-29	-7.441	0.187	V	1
3213.3491	-29	-6.958	0.670	V	1
3211.6295	-29	-8.678	-1.049	V	1
3213.1512	-29	-7.156	0.472	V	1
3570.8060	-22	-6.562	-0.873	V	1
3572.1885	-22	-5.180	0.510	V	1
3571.5086	-22	-5.860	-0.170	V	1
3928.4599	-15	-5.969	-2.218	V	1
3929.3315	-15	-5.097	-1.347	V	1
3931.9234	-15	-2.505	1.245	V	1
3931.2237	-15	-3.205	0.545	V	1
3931.2279	-15	-3.201	0.550	V	1
3930.9966	-15	-3.432	0.318	V	1
3933.5099	-15	-0.919	2.832	V	1
4596.5385	-2	-1.003	-0.854	V	2
4598.4954	-2	0.954	1.103	V	2
4647.7061	-1	-0.844	-0.972	V	2
4647.7223	-1	-0.828	-0.956	V	2
4648.7162	-1	0.166	0.038	V	2
4649.0758	-1	0.525	0.398	V	2
4648.4924	-1	-0.058	-0.186	V	2
4650.1126	-1	1.562	1.435	V	2
4648.7959	-1	0.246	0.118	V	2
4699.6132	0	0.054	-0.350	V	2
4699.6096	0	0.051	-0.354	V	2
4750.8100	1	0.242	-0.439	V	2
4751.4869	1	0.919	0.238	V	2

Ref: (1) Antipin, Sokolovski & Ignatieva (2007), (2) This study

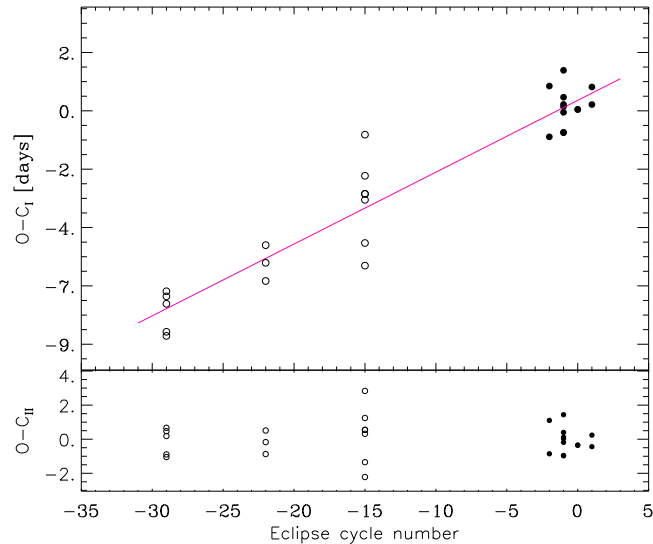


Figure 3. The O-C residuals obtained by Eq.3 for eclipsing binary TYC 1031 1262 1 and a linear least squares fit to the data. The deviations from the fit are plotted in the bottom panel. Open circles refer to the data Antipin, Sokolovski & Ignatieva (2007) and the dots to this study.

4 ANALYSIS

4.1 Effective temperature of the primary star

We have used our spectra to reveal the spectral type of the primary component of TYC 1031 1262 1. For this purpose we have degraded the spectral resolution from 7 000 to 3 000 by convolving them with a Gaussian kernel of the appropriate width, and we have also measured the equivalent widths (EW) of the photospheric absorption lines for the spectral classification. We have followed the procedures of Hernández et al. (2004), choosing helium lines in the blue-wavelength region, where the contribution of the secondary component to the observed spectrum is almost negligible. From several spectra we measured $EW_{\text{HeI}+\text{FeI}\lambda 4922} = 0.81 \pm 0.07 \text{ \AA}$, $EW_{\text{HeI}+\text{FeI}\lambda 4144} = 0.33 \pm 0.05 \text{ \AA}$, $EW_{\text{CaI}\lambda 5589} = 0.35 \pm 0.07 \text{ \AA}$, $EW_{\text{CaI}\lambda 6162} = 0.35 \pm 0.07 \text{ \AA}$ and $EW_{\text{CH(G-band)}\lambda 4300} = 1.05 \pm 0.02 \text{ \AA}$. From the calibration relations EW -Spectral-type of Hernández et al. (2004), we have derived a spectral type of F8 II for the more luminous star with an uncertainty of about 1 spectral subclass. In Fig. 4 we compare spectrum of the variable, obtained on JD 24 55 864, with the spectra of some standard stars.

We have also observed the variable and comparison stars with the standard stars at the same nights. Peak to peak light and color variations of the pulsating star in V, B-V and V-R are about 0.45, 0.14 and 0.09 mag, respectively. The average standard magnitudes and colors of the variable are obtained as $\langle V \rangle = 11.64 \pm 0.04$, $\langle B-V \rangle = 0.77 \pm 0.06$ and $\langle V-R \rangle = 0.50 \pm 0.05$ mag. Comparing the location of the variable in the (B-V)-(V-R) diagram given by Drilling & Landolt (2000) we estimate a spectral type of F8-9 II which is in a good agreement with that derived from spectroscopy. The observed infrared colors of $J-H = 0.368 \pm 0.033$ and $H-K = 0.106 \pm 0.033$ are obtained using the JHK magnitudes given in the 2MASS catalog (Cutri et al. 2003). These colors correspond to a reddened $F9 \pm 2$ supergiant star (Tokunaga 2000) which is consistent with that estimated both from the spectra and BVR photometry.

The effective temperature deduced from the calibrations of Drilling & Landolt (2000), de Jager & Nieuwenhuijzen (1987), Flower (1996), Straižys & Kurielene (1981) and Vitense (1981) are $5\,750 \pm 190 \text{ K}$, $5\,740 \pm 180 \text{ K}$, $5\,970 \pm 228 \text{ K}$, $6\,000 \pm 150 \text{ K}$, and $5\,830 \pm 180 \text{ K}$, respectively. The standard deviations are estimated from the spectral-type uncertainty. The weighted mean of the effective temperature was obtained for the primary star as $5\,880 \pm 165 \text{ K}$. Therefore, an interstellar reddening of $E(B-V) = 0.21$ mag is estimated from the tables given by Drilling & Landolt (2000).

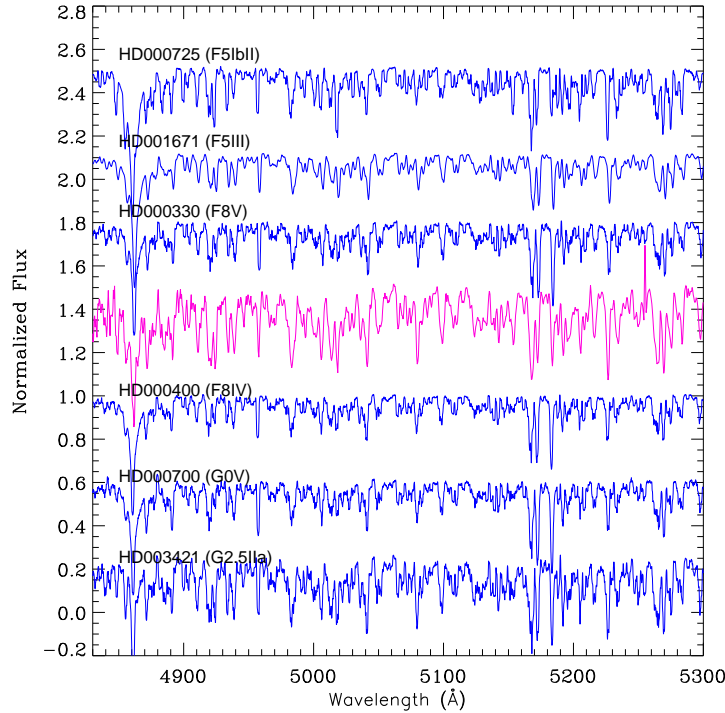


Figure 4. Comparison of the spectrum of TYC 1031 1262 1 with some standard stars with similar spectral type but different luminosity.

4.2 Radial velocities

To derive the radial velocities of the components, the 9 TFOSC spectra of the eclipsing binary were cross-correlated against the spectrum of GJ 182, a single-lined M0V star, on an order-by-order basis using the FXCOR package in IRAF. The majority of the spectra showed two distinct cross-correlation peaks in the quadrature, one for each component of the binary. Thus, both peaks were fitted independently in the quadrature with a *Gaussian* profile to measure the velocity and errors of the individual components. If the two peaks appear blended, a double Gaussian was applied to the combined profile using the *de-blend* function in the task. For each of the 9 observations we then determined a weighted-average radial velocity for each star from all orders without significant contamination by telluric absorption features. Here we used as weights the inverse of the variance of the radial velocity measurements in each order, as reported by FXCOR. We adopted a *two – Gaussian* fit algorithm to resolve cross-correlation peaks near the first and second quadratures when spectral lines are visible separately.

The heliocentric radial velocities for the primary (V_p) and the secondary (V_s) components are listed in Table 4, along with the dates of observations and the corresponding orbital phases computed with the new ephemeris given in previous section. The radial velocities are plotted against the orbital phase in Fig. 5. The velocities in this table have been corrected for the heliocentric

Table 4. Heliocentric radial velocities of TYC 1031 1262 1. The columns give the heliocentric Julian date, the orbital phase (according to the ephemeris in Eq. 3), the radial velocities of the two components with the corresponding standard deviations.

HJD 2400000+	Phase	Star 1		Star 2	
		V_p	σ	V_s	σ
55747.4884	0.4253	4.1	3.5	29.7	4.2
55751.3090	0.4998	2.0	3.3	—	—
55796.2974	0.3770	-5.9	5.4	45.9	5.6
55800.3794	0.4566	5.4	3.5	22.7	4.8
55835.3002	0.1375	-7.7	3.6	48.8	3.6
55864.2074	0.7011	35.8	3.4	-35.9	4.8

reference system by adopting a radial velocity of 14 km s^{-1} for the template star GJ 182. The radial velocities listed in Table 4 are the weighted averages of the values obtained from the cross-correlation of orders #4, #5, #6 and #7 of the target spectra with the corresponding order of the standard star spectrum. The weight $W_i = 1/\sigma_i^2$ has been given to each measurement. The standard errors of the weighted means have been calculated on the basis of the errors (σ_i) in the velocity values for each order according to the usual formula (e.g. Topping (1972)). The σ_i values are computed by FXCOR according to the fitted peak height, as described by Tonry & Davis (1979). The observed radial velocities correspond to the pulsation phases of 0.718, 0.627, 0.360, 0.303, 0.608 and 0.484. In these phases the variation in the radius of the primary star due to oscillation is small, therefore, radial velocity changes of the Cepheid caused by the pulsation are ignored. We did not attempt to decompose the radial velocity measurements of the primary star into the pulsation radial velocity and the orbital radial velocity.

First we analyzed the radial velocities for the initial orbital parameters. We used the orbital period held fixed and computed the eccentricity of the orbit, systemic velocity and semi-amplitudes of the radial velocities. The results of the analysis are as follows: $e=0.001\pm0.001$, i.e. formally consistent with a circular orbit, $\gamma=11.07\pm0.85 \text{ km s}^{-1}$, $K_1=27.4\pm1.7$ and $K_2=48.1\pm1.7 \text{ km s}^{-1}$. Using these values we estimate the projected orbital semi-major axis and mass ratio as: $a \sin i = 76.50 \pm 2.44 R_\odot$ and $q = \frac{M_2}{M_1} = 0.570 \pm 0.041$.

4.3 Intrinsic variations of the primary star

The eclipsing binaries provide critical information about the orbital parameters such as orbital inclination, fractional radii, luminosities, ratio of effective temperatures etc. If the eclipsing binary is a double-lined binary, the masses and radii of the component stars can be determined in solar units. Using the inverse-square law one can accurately determine distance to the system which is independent of all distance methods.

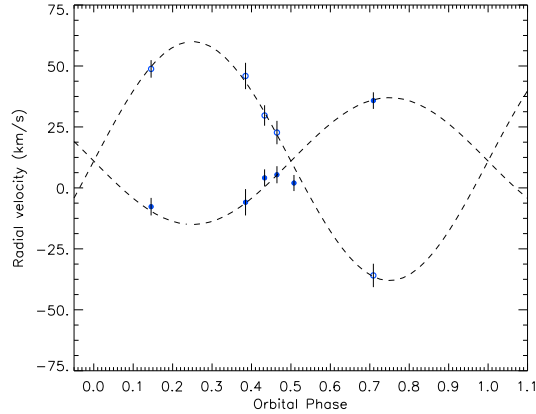


Figure 5. Radial velocities folded on a period of 51.2857 days and the model. Dots (primary) and open circles (secondary) with error bars show the radial velocity measurements for the components of the system

Table 5. Fourier coefficients of the oscillation light curves for TYC 1031 1262 1.

Parameters	<i>B</i>	<i>V</i>	<i>R</i>
A_0	1.0465 ± 0.0022	1.0316 ± 0.0015	1.0016 ± 0.0012
A_1	0.2594 ± 0.0028	0.1948 ± 0.0020	0.1504 ± 0.0016
A_2	0.0543 ± 0.0028	0.0366 ± 0.0020	0.0271 ± 0.0016
B_1	-0.0019 ± 0.0032	0.0123 ± 0.0023	0.0195 ± 0.0018
B_2	-0.0530 ± 0.0031	-0.0371 ± 0.0022	-0.0288 ± 0.0018

The observed light variations are composed of intrinsic light variations of the more luminous star and mutual eclipses. First we subtracted all the observations within the eclipses. The remaining observations are phased with respect to the pulsation period of 4.15270 days. The light curves of the Cepheid show slow decline and rapid rise, i.e., asymmetric light curve with a sharp maximum. The median magnitudes are taken as 12.408, 11.639 and 11.144 mag for B, V and R passbands, respectively. The observed magnitudes are transformed to the flux using the median magnitudes. Then, we represented the intrinsic light variations of the primary star with a truncated Fourier series. Trial-and-error method showed that the observed light curves can well be represented by the second-order Fourier series. The coefficients are given in Table 5 and the fits are compared with the observations in Fig. 6.

4.4 Analyses of the light curves

The intrinsic light variations of the primary star were computed for each oscillation phase using the coefficients given in Table 5. After subtraction of the Cepheid light changes from the observations we obtained light variations, consisting of only from the eclipses and proximity effects. In Fig. 7 the eclipsing light curves in the B, V and R passbands are plotted versus the orbital phases calculated by the ephemeris given in Eq. 3. The light curve of the system with curved maxima

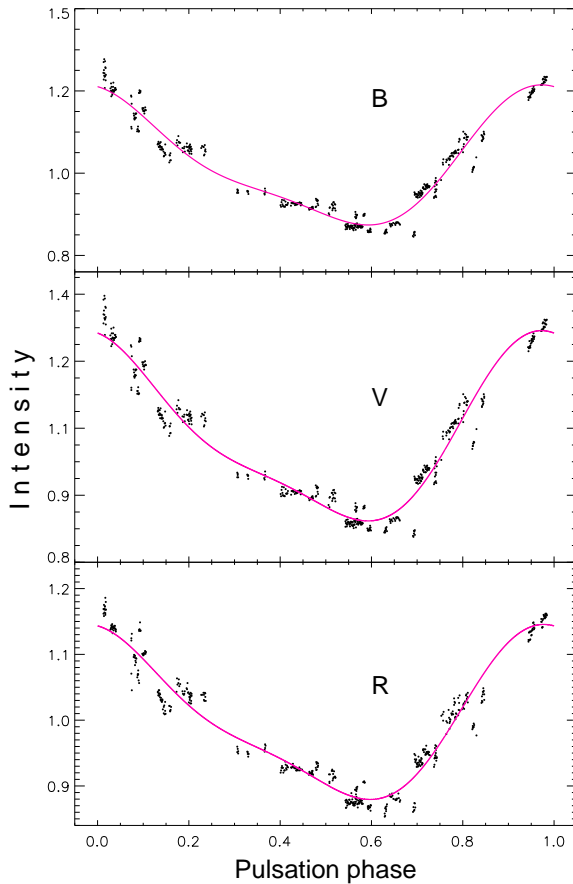


Figure 6. The B, V, and R passbands light curves of the pulsating primary star and their Fourier representations (solid lines) with the coefficients given in Table 5. Note that the ordinates are normalized intensities.

resembles to those β Lyrae-type binaries. The scatter in the binary light curves is mainly caused by the variations in the pulsation period.

We have used the most recent version of the eclipsing binary light curve modeling algorithm of Wilson & Devinney (1971) (with updates, hereafter W-D), as implemented in the PHOEBE code of Prša & Zwitter (2005). It uses the computed gravitational potential of each component to calculate the surface gravities and effective temperatures. The radiative characteristics of the stellar disks are determined using the theoretical Kurucz atmosphere models. The code needs some input parameters, which depend upon the physical properties of the component stars. The U-passband observations are limited and do not cover eclipses, therefore, we excluded these observations from the analysis of light curves for orbital solution.

The BVR photometric observations for the system were analyzed individually. We fixed some parameters whose values were estimated from spectra, such as effective temperature of the hotter component and mass-ratio of the system, which are the key parameters in the W-D code. The effective temperature of the primary star has already been derived from various spectral type-

Table 6. Results of the BVR light curves analyses for TYC 1031 1262 1.

Parameters	<i>B</i>	<i>V</i>	<i>R</i>	Adopted
i°	74.85 ± 0.13	71.26 ± 0.39	76.31 ± 0.49	74.0 ± 0.4
T_{eff1} (K)	5880[Fix]	5880[Fix]	5880[Fix]	5880[Fix]
T_{eff2} (K)	5073 ± 102	4907 ± 72	4661 ± 83	4840 ± 80
Ω_1	3.416 ± 0.037	3.594 ± 0.026	3.709 ± 0.038	3.604 ± 0.033
Ω_2	4.118 ± 0.182	4.054 ± 0.069	4.617 ± 0.100	4.292 ± 0.104
r_1	0.3615 ± 0.0051	0.3380 ± 0.0032	0.3258 ± 0.0042	0.3378 ± 0.0040
r_2	0.1760 ± 0.0101	0.2004 ± 0.0049	0.1839 ± 0.0060	0.1890 ± 0.0064
$\frac{L_1}{(L_1+L_2)}$	0.903 ± 0.015	0.882 ± 0.011	0.892 ± 0.012	
χ^2	2.532	2.186	0.653	
N	972	2557	972	
σ	0.0512	0.0293	0.0260	

effective temperature calibrations as 5 880 K and the mass-ratio from the semi-amplitudes of the radial velocity curves as 0.570. A preliminary estimate for the effective temperature of the cooler component is made using the depths of the eclipses in the BVR passbands. Therefore, initial linear and bolometric limb-darkening coefficients for the primary and secondary components were taken from van Hamme (1993), taking into account the effective temperatures and the wavelengths of the observations. The bolometric albedos were adopted from Lucy (1967) as 0.5, typical for a fully convective stellar envelopes. The gravity-darkening exponents are assumed to be 0.32 for both components, because the stars are cool and are assumed to have convective envelopes. The rotational velocities of the components are assumed to be synchronous with the orbital one. We used Mode 2 of the W-D code which is for detached binaries with no constraints on the potentials. In this mode the fractional luminosity of the secondary component is computed from the other parameters via black body or stellar atmosphere assumption. We assumed synchronous rotation and zero eccentricity.

The adjustable parameters in the differential correction calculation are the orbital inclination, the dimensionless surface potentials, the effective temperature of secondary, and the monochromatic luminosity of the hotter star. Our final results are listed in Table 6 and the computed light curves (continuous line) are compared with the observations in Fig. 7. The secondary minimum appears to be not very well reproduced. This is arisen mainly from the light variation of the pulsating star which is in front of the less massive secondary star at the secondary minimum. We assumed that light variation of the pulsating star is repeated with the same amplitude and the shape of its light curve is not change by time. The uncertainties assigned to the adjusted parameters are the internal errors provided directly by the Wilson-Devinney code. In the last three lines of Table 6 the sums of the squares of residuals (χ^2), number of data points (N) and standard deviations (σ) of the observed light curves are given, respectively. Taking weight inversely proportional to σ , the adopted parameters given in the last column of Table 6 are obtained.

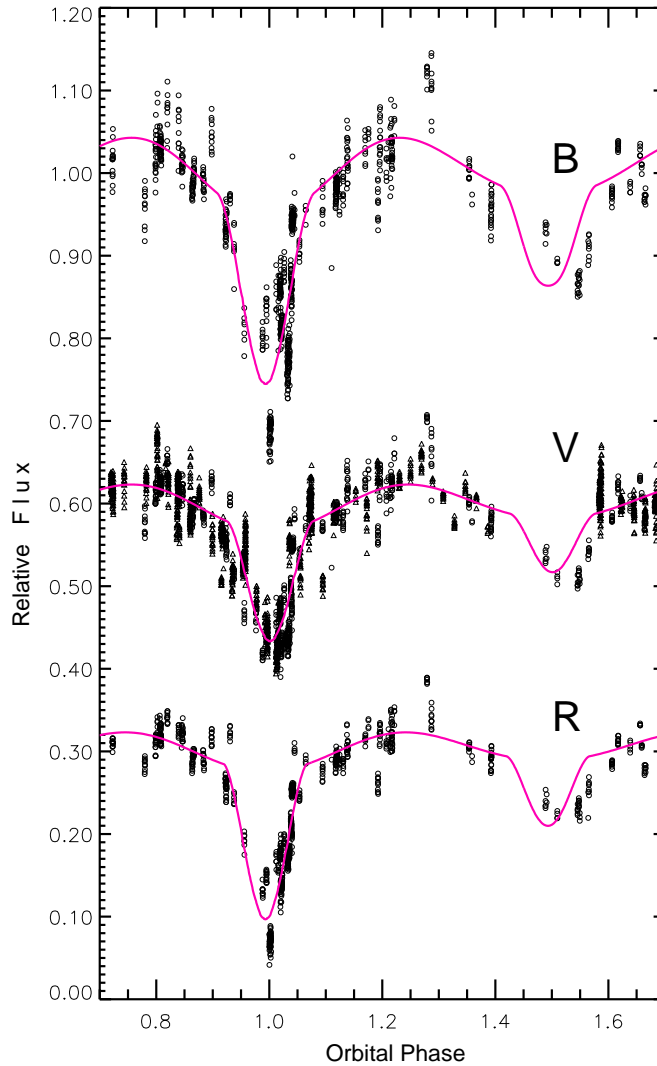


Figure 7. The B, V and R passbands light curves, originated only from the eclipses and proximity effects, and the computed light curves. Circles and dots are for observations obtained by Antipin, Sokolovski & Ignatieva (2007) and in this study and solid lines are for the theoretical curves.

5 RESULTS AND DISCUSSION

A comparison of the results obtained in three light curves reveals some differences in the inclination angle and especially in the fractional radii of the stars. The B and R light curves are constructed by only our own observations. The scatter in the B-passband observations is significantly larger compared to the other bands due to its faintness. Combining the spectroscopic results along with the photometric solutions, listed in the last column of Table 6, the absolute masses, radii, luminosities and surface gravities of the stars are obtained and presented in Table 7. The mass and radius of the pulsating component were determined for the first time directly from radial velocities and multi-color light curves. They are unexpectedly large compared to the Type II Cepheids. The luminosity and absolute bolometric magnitude M_{bol} of each star were computed from their effective temperatures and radii. The bolometric magnitude and effective temperature for the Sun

are taken as 4.74 mag and 5770 K (Drilling & Landolt (2000)). Comparison of its location in the Hertzsprung-Russell diagram (HR), constructed for the metal-poor cepheids by Gingold (1985), their Fig. 1, indicates that TYC 1031 1262 1 is in the instability strip of the Type II Cepheids, about 20 times more luminous than the RR Lyrae stars. It seems to have the same luminosity and effective temperature with the Type II Cepheids having pulsation periods of about 10 days, closer to the blue edge of the IS. When we compare with the solar composition models, for example Baraffe et al. (1998), the primary star appears to be an evolved $5 M_{\odot}$ star and the secondary is consistent with an evolved $3 M_{\odot}$ star.

After applying bolometric corrections to the bolometric magnitudes, we obtained absolute visual magnitudes of the components. Taking into account the light contributions of the stars and total apparent visual magnitude we calculated their apparent visual magnitudes. The light contribution of the secondary star $L_2/(L_1+L_2)=0.02, 0.04$ and 0.08 are obtained directly from the B-, V-, and R-bandpass light curve analysis, respectively. This result indicates that the light contribution of the less massive component is very small, indicating its effect on the color at out-of-eclipse is almost negligible for the shorter wavelengths. For the bolometric corrections given by (Drilling & Landolt (2000)) we calculated the distance to TYC 1031 1262 1 as $d=5074\pm 207$ pc. However the infrared JHK magnitudes give a distance of 5040 ± 255 pc. Estimating distances to the stars are strongly depended on the bolometric corrections. If we adopt the bolometric corrections given by Code et al. (1976) and Bessell, Castelli & Plez (1998), the distances to TYC 1031 1262 1 are obtained as 5082 ± 540 , and 5110 ± 650 pc, respectively. The average distance to the system was obtained as 5070 ± 250 pc. The distance from the galactic plane is calculated as 970 pc using its galactic latitude of 11 degrees, about 14 times larger than the mean scale height of the Type I Cepheids. We have calculated Galactic space-velocity components of the system using the coordinates, distance, systemic radial velocity, and proper motions and listed in the last line of Table 7. The U, V, and W are velocities toward the galactic center, toward the direction of galactic rotation and toward the north galactic pole, respectively. With planer and vertical eccentricities of 0.50 and 0.26 and the velocity components the system is most probably belonging to the thick-disk population. This result confirms the earlier suggestion of Harris & Wallerstein (1984) that many field Type II Cepheids are metal rich and have kinematic properties similar to the old-disk or thick-disk population.

The pulsation period of TYC 1031 1262 1 has shown a secular period increase with an amount to $2.46 (\pm 0.54) \text{ min yr}^{-1}$. Vinko, Szabados & Szatmary (1993) investigated secular period change in AU Peg, another Type II Cepheid which belongs to a binary system. The observed rate of the pe-

Table 7. Fundamental parameters of TYC 1031 1262 1.

Parameter	TYC 1031 1262 1	
	Primary	Secondary
Spectral Type	F8(± 1)II	G6(± 1)II
Mass (M_{\odot})	1.640 \pm 0.151	0.934 \pm 0.109
Radius (R_{\odot})	26.9 \pm 0.9	15.0 \pm 0.7
T_{eff} (K)	5880 \pm 200	4890 \pm 125
Luminosity (L_{\odot})	764 \pm 144	109 \pm 26
Gravity(<i>cgs</i>)	62 \pm 3	114 \pm 11
a (R_{\odot})	79.58 \pm 2.54	
V_{γ} (km s^{-1})	11.07 \pm 0.85	
i ($^{\circ}$)	74.0 \pm 0.4	
q	0.570 \pm 0.041	
d (pc)	5070 \pm 250	
$\mu_{\alpha} \cos \delta, \mu_{\delta}$ (mas yr^{-1})	2.7 \pm 0.8, 0.8 \pm 0.8	
U, V, W (km s^{-1})	-14.5 \pm 13.0, 47.7 \pm 14.9, -47.2 \pm 19.1	

riod increase in TYC 1031 1262 1 is about 5 times larger than that of AU Peg. McCharty & Nemec (1997) observed a decrease in the pulsation period of V19 in the globular cluster NGC 5466 which is known as an AC with a mass of 1.66 M_{\odot} and a pulsation period of 0.82 d. They propose that this would be an indication of blueward evolution. In contrary, TYC 1031 1262 1 shows a period increase and its large magnitude should indicate faster evolutionary timescale redward. Sandage, Diethelm & Tammann (1995) and Diethelm (1996) proposed that all of the BL Her Cepheids appear to have increasing periods and are consistent with post-blue horizontal branch models of Population II stars. The observed period increase in TYC 1031 1262 1 appears to confirm this suggestion. Unlike the BL Her Cepheids, the TYC 1031 1262 1 has a companion very close to it. Period change rates are determined for only a few ACs. Yet the cause of such a relatively large pulsation period change in a Type II Cepheid has not been obvious. Observations covering a long time span are crucially needed for better understanding of such a large increase rate in pulsation period in the TYC 1031 1262 1, as well as in other Type II Cepheids.

As it is quoted in §1, Type II Cepheids are divided into three subclasses: BL Her, W Vir, and RV Tau. All three classes are characterized by the presence of Balmer emission, especially $H\alpha$, during some parts of their pulsation cycle. Evolutionary scheme of these classes is suggested by Gingold (1985). In this scheme the BL Her stars are evolving from horizontal branch towards the lower asymptotic giant branch. However, the W Vir variables are on loops to the blue from the asymptotic giant branch. The RV Tau stars are moving to the blue in a post-asymptotic giant branch phase. He investigates evolutionary status of Type II Cepheids as post-horizontal-branch stars and calls attention to a different structure and evolution of the ACs. He estimates masses of Type II Cepheids around 0.6 M_{\odot} with a radius of about 8 R_{\odot} in the post-horizontal-branch phase. Bono, Caputo & Santolamazza (1997a) suggest masses between 0.52 and 0.59 M_{\odot} for the Type II

Cepheids using their pulsation properties rather than evolutionary tracks. Now there is a consensus that Type II Cepheids are fundamental pulsators with masses below $0.8 M_{\odot}$.

With a mass of about $1.640 M_{\odot}$, luminosity of $760 L_{\odot}$ and radius of $27 R_{\odot}$ the pulsating primary component of TYC 1031 1262 1 cannot be a Type II Cepheid. If it were a Type I Cepheid its mass would be greater than $4 M_{\odot}$ according to the models given by Bono, Castellani & Marconi (2000) for $Z=0.02$ and even for $Z=0.004$. However the ACs are usually accepted to be metal-poor horizontal branch stars with masses above $1.5 M_{\odot}$. Soszynski et al. (2008) presented 83 ACs in the Large Magellanic Cloud and showed that ACs are located between Type I and Type II Cepheids in the P-L diagram. They are found in every dwarf spheroidal galaxy, and unlike Type II Cepheids, are absent in globular clusters, except a few ACs in ω Cen. Demarque & Hirschfeld (1975) propose for their origin that they are young single stars due to recent star formation. In contrary, Renzini, Mengel & Sweigart (1977) suggest that they are formed as a consequence of mass transfer in binary systems with the same age of the stellar systems they belong. Bono, Caputo & Santolamazza (1997b) examined evolution and pulsation properties of ACs and concluded that models of masses between 1.5 and $2.2 M_{\odot}$ fit most of the stars. Concerning the origin of ACs, as single young stars or old binary systems, they have noted that their results did not support a single interpretation. The mass, luminosity, kinematic properties and light curves of TYC 1031 1262 1 fulfil most of the properties of the Anomalous Cepheids. As pointed out by Soszynski et al. (2008) and Fiorentino & Monelli (2012) the mode identification of an AC is very complex and can not be based only on their light curves. However, Soszynski et al. (2008) compared light curves of the ACs in the LMC. They proposed that the ACs pulsating in the first overtone have generally smoother light curves than for the fundamental-mode pulsators with rounded maxima and minima. The shape of the light curve of the pulsating star looks like to those of fundamental-mode pulsators. If we compare its location on the $M_V - \log P$ plane given by Fiorentino & Monelli (2012) for the ACs in the LMC, whose pulsating periods are shorter than 2.4 d, the pulsating star is located on the extension of fundamental - pulsators, as though its classification as a fundamental-pulsator is supported. In Fig. 8 we compare position of TYC 1031 1262 1 on the color-magnitude diagram with other ACs taken from Harris, Olszewski & Wallerstein (1984) and Nemec, Nemec & Lutz (1994). It is located among the brightest ACs close to the blue edge, with a luminosity of about 800 times solar. The binary Cepheid ST Pup with a pulsation period of about 18.47 d, is located very close to the TYC 1031 1262 1. In contrary, the binary Cepheids TX Del with a pulsation period of 6.2 d and AU Peg with a period of 2.4 d, are located at the red-edge of the IS, with lower luminosity.

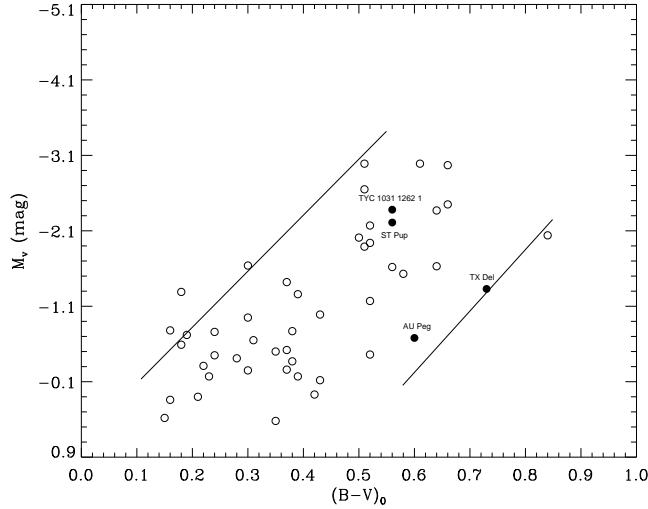


Figure 8. The position of TYC 1031 1262 1 on the color-magnitude diagram. The circles refer to the Type II Cepheids in globular clusters and the dots for TYC 1031 1262 1, ST Pup, AU Peg and TX Del. The lines show the borders of instability strip for Type II Cepheids.

6 CONCLUSIONS

We have obtained multi-color light curves and radial velocities of the eclipsing binary system TYC 1031 1262 1 of which the luminous component is a Cepheid. The astrophysical parameters of the component stars were obtained directly by analysing the light curves and radial velocities. In earlier studies the brighter star was classified as a metal-poor Type II Cepheids. In contrary, some investigators include it into the classical cepheids. The mass of the pulsating primary star with an amount of $1.64 M_{\odot}$ indicates that its structure and evolution are different from those of the RR Lyrae and W Vir stars. The galactic velocity components U , V , W have been determined as -14.5 , 47.7 and -47.2 km s^{-1} and the distance from the galactic plane as about 970 pc. All these properties and the asymmetric pulsating light curve lead us to classify the Cepheid as an Anomalous Cepheid. The pulsation period appears to be increasing with an amount of $2.46 (\pm 0.54) \text{ min yr}^{-1}$, the largest period change observed in the Type II Cepheids so far. This observed increase rate indicates that the star evolves redward in the IS with shorter timescales.

The pulsating primary star fills almost 85 per cent of its corresponding Roche lobe while the less massive star 61 per cent. The pulsating component in TYC 1031 1262 1 is very close to its Roche lobe, therefore, mass loss or transfer to its companion has taken place. Both components are supergiant and the separation is only two times the sum of their radii. The companion should unexpectedly affect both pulsation and evolution of the Cepheid. However, it is not clear how such a close companion can cause any period variation on pulsation by tidal interaction alone. Most of the ACs are faint stars and have relatively longer orbital periods, therefore, measurements of the

radial velocities ACs in binary systems are very difficult. In addition the velocity variations due to the orbital motion may be affected by the pulsation depending on the inclination of the orbits. In the case of TYC 1031 1262 1 the orbital inclination is sufficiently large to separate the orbital velocities of both components. If mass loss or transfer from the pulsating star has taken place, the orbital period of the system would be changed, which can be revealed by the observations to be made in coming years. This will yield us some clues about the further evolution of the ACs in binary systems.

ACKNOWLEDGMENTS

Special thanks goes to Dr. S. Bilir and F. Soyduğan for his valuable suggestions and discussion about the kinematic properties of the system. We thank to TÜBİTAK National Observatory (TUG) for a partial support in using RTT150 telescope with project numbers 10ARTT150-483-0, 11ARTT150-123-0 and 10CT100-101. We also thank to the staff of the Bakırlıtepe observing station for their warm hospitality. This study is partly supported by Turkish Scientific and Technology Council under project number 108T237. The following internet-based resources were used in research for this paper: the NASA Astrophysics Data System; the SIMBAD database operated at CDS, Strasbourg, France; TÜBİTAK ULAKBİM Süreli Yayınlar Kataloğu-TURKEY; and the arXiv scientific paper preprint service operated by Cornell University. The authors are indebted to the anonymous referee for his/her valuable suggestions which improved the paper.

REFERENCES

- Antipin, S. V., Sokolovsky, K. V., & Ignatieva, T. I., 2007, MNRAS, 379, L60-L62
- Baade, W., 1953, Trans. IAU, 8, 398
- Baraffe I., Chabrier G., Allard F., Hauschildt P., 1998, A&A, 337, 403
- Blaauw, A. & Morgan, H. R., 1954, BAN, 12, 95
- Bessell M. S., Castelli F., & Plez B., 1998, A&A, 333, 231
- Bono G., Caputo F., & Santolamazza P., 1997a, A&A, 317, 171
- Bono G., Caputo F., & Santolamazza P., 1997b, AJ, 113, 2209
- Bono G., Castellani V., & Marconi M., 2000, ApJ, 529, 293
- Code A. D., Bless R. C., Davis J., and Brown R. H., 1976, ApJ, 203, 417
- Cutri R. M., et al., 2003, The IRSA 2MASS All-Sky Point Source Catalog, NASA/IPAC Infrared Science Archive. <http://irsa.ipac.caltech.edu/applications/Gator/>

- Demarque, P. & Hirschfeld, A. W., 1975, *ApJ*, 202, 346
- Diethelm, R., 1996, *A&A*, 307, 803
- Drilling J. S., Landolt A. U., 2000, *Allen's astrophysical quantities*, 4th ed. Edited by Arthur N. Cox. ISBN: 0-387-98746-0. Publisher: New York: AIP Press; Springer, 2000, p.381
- Fiorentino G., Limongi M., Caputo F., and Marconi M., 2006, *A&A*, 460, 155
- Fiorentino G., Monelli M., 2012, *A&A*, 540, 102
- Flower P. J., 1996, *ApJ*, 469, 355
- Gingold, R. A., 1985, *Mem.Soc.Astr. Italy*, 56, 169
- Harris, H., 1981, *AJ*, 86, 719
- Harris, H. C., & Wallerstein, G., 1984, *AJ*, 89, 379
- Harris, H. C., Olszewski, E. & Wallerstein, G., 1984, *AJ*, 89, 119
- Hernández J., Calvet N., Briceño C., Hartmann L., Berlind P., 2004, *AJ*, 127, 1682
- de Jager C., Nieuwenhuijzen H., 1987, *A&A*, 177, 217
- Khruslov, A. V., 2008, *PZ*, 28, 4
- Landolt, A. U., 1983, *AJ*, 88, 439
- Landolt, A. U., 1992, *AJ*, 104, 340
- Lenz, P. & Breger, M., 2005, *CoAst*, 146, 53
- Lucy L. B., 1967, *Z. Astrophys.*, 65, 89
- McCharty, J. K. & Nemec, J. M., 1997, *ApJ*, 482, 203
- Nemec, J. M., Nemec, A. F. L. & Lutz, T. E., 1994, *AJ*, 108, 222
- Nidever D. L., Marcy G. W., Butler R. P., Fischer D. A., and Vogt S. S., 2002, *ApJS*, 141, 503
- Pojmanski, G., Pilecki, B. & Szczygiel, D., 2005, *AcA*, 55, 275
- Prša A., Zwitter T., 2005, *ApJ*, 628, 426P
- Renzini, A., Mengel, J. G., & Sweigart, A., 1977, *A&A*, 56, 369
- Sandage, A., Diethelm, R. & Tammann, G. A., 1995, *A&A*, 283, 111
- Schmidt, E. G., Hemen, B., Rogalla, D., & Thacker-Lynn, L., 2009, *AJ*, 137, 4598
- Soszynski, I., Udalski, A. Szymanski, M. K. et al., 2008, *AcA*, 58, 293
- Straizys, V. & Kuriliene, G., 1981, *ApSS*, 80, 353
- Tokunaga A. T., 2000, "Allen's astrophysical quantities", Fourth Edition, ed. A.N.Cox (Springer), p.143
- Tonry, J., & Davis M., 1979, *AJ* 84, 1511
- Topping J., 1972, "Errors of Observation and Their Treatment", (Chapman and Hall Ltd.), p.89
- van Hamme, W. 1993 *AJ*, 106, 2096

Vinko J., Szabados L., & Szatmary K., 1993, *A&A*, 279, 410

Vitense, E. B., 1981, *ARA&A*, 19, 295

Wallerstein, G., 2002, *PASP*, 114, 689

Wilson R.E. & Devinney E.J., 1971, *ApJ*, 166, 605

Wozniak, P. R., Vestrand, W. T. Akerlof, C. W. et al., 2004, *AJ*, 127, 2436

